Two distinct Sb-adsorption steps on Si(5 5 12)-2×1: Indiffusion followed by preferential adsorption

Huiting Li, Y.-N. Xu, Y.-Z. Zhu, Hidong Kim, and Jae M. Seo*
Department of Physics and Institute of Photonics and Information Technology, Chonbuk National University, Jeonju 561-756, Korea
(Received 5 January 2007; revised manuscript received 1 May 2007; published 25 June 2007)

Initial stages of antimony (Sb) adsorption on the Si(5 5 12)-2×1 surface have been studied by scanning tunneling microscopy in order to understand interfacial reaction between adsorbed Sb atoms and the Si template with one-dimensional (1D) symmetry. It has been found that there are two distinct steps, Sb indiffusion and preferential adsorption, at the initial Sb adsorption on Si(5 5 12)-2×1 held at 600 °C. Initially, deposited Sb atoms diffuse into the subsurface, cause indirect Si deposition, and result in surface reconstruction from a (5 5 12) terrace to (337) terraces with (113) steps. As soon as the subsurface Sb sites are saturated by indiffused Sb atoms, additionally deposited Sb atoms are preferentially adsorbed along the upper (113)-step edges and form 1D Sb wires with a spacing of about 10 nm, which corresponds to two periodic lengths of the original (5 5 12) surface. Once Sb-adsorption sites, (113) steps, are saturated, deposited Sb atoms cluster for themselves and do not contribute to nanowire fabrication. From the present studies, it has been found that both Sb indiffusion and preferential adsorption stabilize the high-index surface through relieving surface strain by way of either inserting or attaching Sb atoms, but once such surface strain is relieved, the 1D growth mode also terminates.

DOI: 10.1103/PhysRevB.75.235442 PACS number(s): 68.43.Jk, 68.37.Ef, 68.35.Ct

I. INTRODUCTION

In order to grow nanostructures on a large scale and apply them to nanodevices of high density, first of all, a well-defined template to a nanometer scale should be prepared. One of the potential templates to satisfy such a goal is the high-index Si(5 5 12)-2×1 surface, since it is reconstructed to a planar surface having a single domain with one-dimensional (1D) symmetry and a relatively large unit cell of 5.35×0.77 nm^2. Up to now, several structural models of Si(5 5 12)-2×1 have been proposed.[1–3] Even if its detailed atomic structure is still under controversy, the common point of these models is that one unit period of Si(5 5 12)-2×1 consists of two kinds of (337) units and one (225) unit, and that these units are separated by chain structures. Most recently, it has been reported that these subunits are composed of stable 1D structures along the $[1\bar{1}0]$ direction, such as a dimer-adatom (D-A) row, a tetramer (T) row, a honeycomb (H) chain, and a 6-5-ring π-bonded (π) chain.[4] Therefore, if there exists a preferential adsorption site among these 1D structures during deposition of metal atoms, metal nanowires with a spacing of about 5 nm can be possibly formed on a large scale.

Nevertheless, due to instability of high-index Si surfaces, most of them are easily faceted by adsorbing metal atoms and/or thermal heating.[5] For example, the Au/Si(5 5 12)-2×1 systems studied by Baski *et al.* using scanning tunneling microscopy (STM) have shown that the Si(5 5 12)-2×1 surface is faceted to (113), (225), (337), (5 5 11), and (7 7 17) terraces by adsorbed Au.[6] In the Bi/Si(5 5 12)-2×1 system studied by Cho and Seo using STM, it has also been reported that the reconstructed (5 5 12) terrace is converted to (337) terraces at the initial Bi-adsorption stage.[7] More recently, in the Sb/Si(5 5 12)-2×1 system studied by Kumar *et al.* using low energy electron diffraction (LEED), it has been reported that the (5 5 12) surface is transformed to different kinds of facets, such as (225), (337), and (113), depending on Sb coverage and substrate temperature.[8,9] In the present study, based on the known atomic structure of Si(5 5 12)-2×1 surface, the detailed adsorption steps of the Sb/Si(5 5 12)-2×1 system have been identified by STM in order to understand such an initial faceting process of the high-index Si substrate and find the possibility of 1D growth of metal atoms on this template.

II. EXPERIMENT

The experiments were carried out in an ultrahigh vacuum (UHV) chamber with a base pressure of 2.0×10^{-10} Torr. A Si(5 5 12) substrate with a size of $3\times13\times0.25$ mm^3 was cut from an *n*-type (P-doped) Si wafer. After degreasing with pure organic solvents in the air, it was mounted on a Mo holder, transferred to a UHV chamber, and outgassed for 24 h at 650 °C. The reconstructed Si(5 5 12)-2×1 surface was prepared through resistive heating at 1200 °C followed by slow cooling from 900 to 550 °C at a rate of 10 °C/min. Sb atoms were thermally evaporated on the reconstructed Si(5 5 12)-2×1 surface held at 600 °C at a rate of 0.05 monolayer (ML)/min. Since one (5 5 12) unit is composed of seven bilayer steps, 28 atoms per unit cell (i.e., 6.8×10^{14} atoms/cm^2) are needed to cover the surface.[10] So, in the present article, 1 ML is defined as 6.8×10^{14} atoms/cm^2. All STM images were acquired with constant current mode at room temperature.

III. RESULTS AND DISCUSSION

A. Atomic structure of the Si(5 5 12)-2×1 surface

Scanning tunneling microscopy images of the reconstructed Si(5 5 12)-2×1 surface and the corresponding top- and side-view structural models employed in the present Sb-

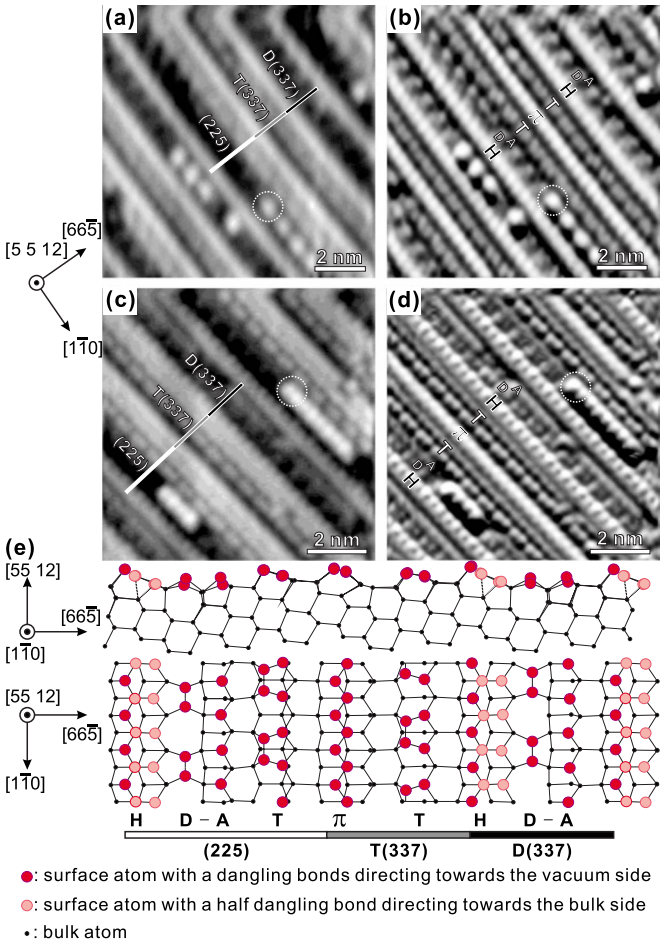

FIG. 1. (Color online) STM images and structural model of the reconstructed Si(5 5 12)-2×1 surface. (a) Filled-state (V_{sample} =−2 V) and (c) empty-state (V_{sample}=+2 V) topographic images. Size: 10×10 nm^2 and I_t=0.5 nA. One unit of Si(5 5 12)-2×1 is composed of (225), T(337), and D(337) subunits. [(b) and (d)] Corresponding error-signal images of (a) and (c), respectively. H, π, T, and D-A indicate honeycomb chain, π-bonded chain, tetramer row, and dimer-adatom row, respectively. One of addimers is encircled in (a)–(d). (e) Side and top views of the Si(5 5 12)-2×1 structural model.

adsorption studies are shown in Fig. 1.[4] In order to differentiate one kind of 1D feature from another, a filled-state topographic image and the error-signal image are presented in Figs. 1(a) and 1(b) and an empty-state topographic image and the error-signal image are presented in Figs. 1(c) and 1(d). Topographic images show the z height and error-signal images show the edges of features more clearly by recording the difference between the set current and the actually measured current controlling the z-axis motion in the feedback mode.[11] As designated by line segments in Figs. 1(a) and 1(c), one periodic unit along the [66$\bar{5}$] direction is composed of one (225) subunit and two kinds of (337) subunits. The 1D chain structures appear to be brighter than the neighboring features in all the STM images shown in Figs. 1(a)–1(d).[1–4] It should be noted that these chain structures, which appear to be identical in the filled-state images of Figs. 1(a) and 1(b), are clearly not of a kind, as shown in the empty-state images of Figs. 1(c) and 1(d). Among the three chain structures in one periodic unit, two of them showing fluctuating brightness in Figs. 1(c) and 1(d) have the H chain structure, while the one left without fluctuating brightness is the π chain structure with 6-5-member rings.[4] Besides the chain structures, as shown in Fig. 1(d), one of the 1D structures with a 2× periodicity along the [1$\bar{1}$0] direction is the T row existing at both sides of a π chain and the other is the D-A row having additionally adsorbed species. One (337) subunit designated by a gray bar in Figs. 1(a) and 1(c) is the T(337) composed of a π chain and a T row as shown in Figs. 1(b) and 1(d). The other (337) subunit designated by a black bar is the D(337) composed of an H chain and a D-A row. A T(337) can be transformed to a D(337) under tensile stress.[7,10] The (225) subunit designated by a white bar is composed of an H chain, a D-A row, and a T row, so it can be considered as a composition of a D(337) subunit and a T row [or a (113) subunit].

As seen inside the dotted circles of Figs. 1(a)–1(d), an adsorbed species is detected only from D-A rows. Compared with T or D-A structures having a 2× periodicity, a protrusion of this adsorbed species seems to have a maximum with a 2× periodicity along the D-A row in the filled-state image of Fig. 1(b), while it has a pair of maxima with a 1× periodicity in the empty-state image of Fig. 1(d). This implies that the adsorbed species is a Si dimer mostly aligned to the [1$\bar{1}$0] direction. Also, this indicates that the unique adsorption site for Si dimers is a D-A row among the four kinds of 1D structures. Therefore, such a deduction provides the criterion in determining the atomic structure underneath the adsorbed species. It has also been reported that transformation from T(337) to D(337) is a prerequisite condition for an additional Si dimer to be adsorbed on the original T(337) subunit site during Si homoepitaxy on the Si(5 5 12)-2×1 surface.[10]

In Fig. 1(e), the structural model of the reconstructed Si(5 5 12)-2×1 surface, deduced from the STM images of Figs. 1(a)–1(d), is shown.[4] Four kinds of 1D structures, such as T row, D-A row, H chain, and π chain, have the identical number of dangling bonds per unit period along the [1$\bar{1}$0] direction. From the previous reports of Si homoepitaxy on Si(5 5 12)-2×1, it has been found that these 1D structures transform among themselves.[10] For example, adsorbed dimers on a D-A row transform to a chain structure, a chain structure is transformed to a T row by the external compressive stress, and a T row is converted to a D-A row by the external tensile stress. All of these results and the STM images shown in Figs. 1(a)–1(d) commonly manifest the fact that only four kinds of 1D structures can exist on the Si(5 5 12)-2×1 surface in the order of [H+D-A+T]+[π +T]+[H+D-A] in one periodic unit along the [66$\bar{5}$] direction as shown in Fig. 1(e)

B. Preferential adsorption of outdiffused Si atoms and structural transformations by Sb indiffusion

In Fig. 2(a), a topographic STM image, obtained from Si(5 5 12) after deposition of 0.01 ML of Sb on the recon-

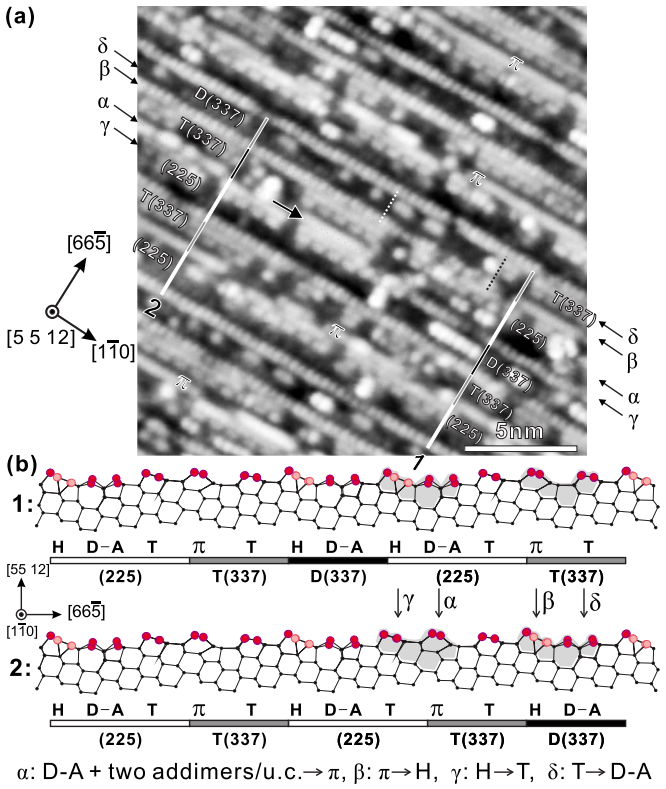

FIG. 2. (Color online) STM image obtained from the Si(5 5 12)-2×1 surface deposited with 0.01 ML of Sb at substrate temperature of 600 °C and corresponding structural model of segment 1 and segment 2. (a) Empty-state (V_{sample}=+1.4 V) topography image. Size: 20×20 nm^2 and I_t=0.5 nA. The black arrow inside the image points the growth direction of a new chain. π's inside the image indicate π-bonded chains. The black dotted line is the boundary between T(337) and D(337). (b) Side-view models corresponding to segment 1 and segment 2.

structed Si(5 5 12)-2×1 substrate held at 600 °C, is presented. From Fig. 2(a), a new 1D chain, which appears to be identical with pre-existing π chains with a 1× periodicity, is detected. This chain is growing on the D-A row in a (225) subunit from the top-left side along the direction designated by a black arrow inside the image.

According to previous reports on Sb adsorption on low-index Si surfaces, Sb atoms are preferentially adsorbed as an addimer as long as the adsorption sites are provided.[12–14] Although either Sb dimers or Si dimers can be adsorbed on the D-A row, it turns out that only Si dimers can be adsorbed sequentially on the D-A row to form a chain structure due to difference between the bond length of an Sb dimer (2.9 Å) and that of a Si dimer (2.4 Å).[15] If Sb dimers are adsorbed sequentially on the D-A row, they will apply more compressive stress on the Si substrate due to lattice mismatch. So, the stable and long Sb addimer row, which will be a precursor for a chain structure, cannot be formed at this stage. In addition, if this new chain is composed of Sb with five electrons in the outermost shell instead of Si with four valence electrons, the empty-state image will show the STM image quite different from that of the pure Si surface, since the Sb atoms have three-bonding configuration and one occupied lone pair orbital.[16] Therefore, such a new chain structure shown in Fig. 2(a) is composed of Si atoms, which are indirectly deposited as a result of Sb diffusion into the substrate held at 600 °C. In order to observe the relation between Sb coverage and the newly formed chain in (225), the coverage of this new chain in (225) has been measured from the STM images (not shown here). When 0.005 and 0.01 ML of Sb atoms were deposited, it was measured that 2.3% and 5.0% of the D-A sites in (225)'s were covered with newly formed chains, respectively. In principle, at 1/7 ML of Si coverage, all of the D-A sites in (225)'s can be covered with new chains. So, if all the deposited Sb atoms substitute Si atoms and all the substituted Si atoms form chains on the D-A sites in (225)'s, at 0.005 and 0.01 ML of Sb coverage, it has been estimated that 3.4% and 6.9% of the D-A sites in (225)'s should be covered with new chains, respectively. The difference between the estimated coverages and the measured ones from STM images is due to growth of Si structures at facets which are not parallel to the [1$\bar{1}$0] direction, which will be shown in Fig. 4(a). The similar indirect deposition during deposition of metals diffusing into the Si substrate held at elevated temperatures was also reported.[17–19] For example, Garni *et al.* reported that, as a result of Sb deposition on Si(001) at 302 °C, only the siliconlike islands are observed above the surface[20] and Saranin *et al.* reported that, as a result of Sb deposition on Si(100), the surface becomes rough due to indirect deposition of Si caused by Sb indiffusion.[21]

In order to understand the detailed structural transformation due to this 1D feature, two adjoining areas of the same width, marked by line segments "1" and "2" in Fig. 2(a), are analyzed using the structural information of Si(5 5 12)-2×1 shown in Fig. 1. The subunit ordering in segment 1 along the [66$\bar{5}$] direction, (225)-T(337)-D(337)-(225)-T(337), has been altered to the subunit ordering in segment 2, (225)-T(337)-(225)-T(337)-D(337), by Sb deposition. Such an alteration of subunit ordering originates from a new π chain structure formed on the D-A row, designated by α, in the (225) subunit of the original surface. Due to this new chain, the original (225) and its adjacent D(337) subunits in segment 1 are converted to T(337) and (225) subunits in segment 2, as shown in Fig. 2(a) In addition to this kind of subunit switching, alteration within the original T(337) subunit adjacent to the original (225) subunit, that is, conversion from T(337) to D(337), has been found, as confirmed by addimers in it, since dimers can be adsorbed only on the D-A row, not on the T row.[10] Using the atomic structure of each subunit shown in Fig. 1(e), the structural models corresponding to two segments, 1 and 2, are drawn in Fig. 2(b). It can be easily found that there are four kinds of 1D structural transformations (indicated by α, β, γ, and δ) related to a new chain structure on the D-A row in the original (225) subunit. In the structural transformations indicated by α and γ, there is a change in the number of surface atoms per unit cell from seven pairs [i.e., the surface atoms with the left-hand gray background of segment 1 in Fig. 2(b)] to nine pairs [those of segment 2], which results from indirect deposition of Si atoms. It therefore needs two Si dimers per unit cell in order to form a new chain. While two Si dimers per unit cell are

adsorbed on the D-A row and form a new π chain structure (designated by α), the compressive stress is applied to the neighboring H chain along the $[\bar{6}\bar{6}5]$ direction and converts it to a T row (designated by γ). In the previous study of Si homoepitaxy on Si(5 5 12)-2×1,[10] Kim *et al.* also reported that two Si dimers per unit cell adsorbed on a D-A row transform to a chain structure while one addimer per unit cell remains as a dimer row. Due to formation of a new chain structure, two sequential T(337) subunits become unstable and transform to D(337)+T(337) through splitting a T row to a D-A row (designated by δ) as well as transforming a π chain to an H chain (designated by β). As can be seen in Fig. 2(a), in the case of Sb deposition, differently from homoepitaxy, the conversion from T(337) to D(337) advances the formation of a new π chain by about 5 nm along the $[1\bar{1}0]$ direction. In Fig. 2(a), the black dotted line is the boundary between T(337) and D(337) and the white dotted line indicates the place where the conversion should happen in the case of homoepitaxy on Si(5 5 12)-2×1. The reason is also thought to be due to tensile stress induced by the indiffusion of Sb atoms, the atomic radius of which (1.45 Å) is larger than that of Si (1.10 Å). These transformations of β and δ are just rebondings among surface atoms, as can be seen in the right-hand gray backgrounds of segments 1 and 2 in Fig. 2(b).

It can be deduced from the result shown in Fig. 2 that, at the initial stage of Sb adsorption on the Si(5 5 12)-2×1 substrate at elevated temperature, deposited Sb atoms diffuse into the substrate and replace subsurface Si atoms. The replaced Si atoms are outdiffused and adsorbed preferentially on the D-A sites in the (225) subunit to form a new π chain, which always causes structural transformations of neighboring 1D structures through simple rebonding processes.

Scanning tunneling microscopy images, obtained from the Si(5 5 12)-2×1 surfaces deposited with 0.05 and 0.1 ML of Sb at substrate temperature of 600 °C, are shown in Figs. 3(a) and 3(b) and Figs. 3(c) and 3(d), respectively. In Fig. 3(a), most of a (5 5 12) terrace has been converted to (337) terraces. Using the result of the LEED and electron energy loss spectroscopy features, Kumar *et al.* reported that when Sb atoms are deposited on the Si(5 5 12) surface held at 680 °C, the (337) terraces are formed.[8] From adsorbed addimers, it can be realized that all of the (337) subunits are homogeneous D(337) ones. Besides (337) terraces, the step indicated by an upward white arrow is also shown in Fig. 3(a), a filled-state image of a large area. Figure 3(b), an empty-state image of a small area, shows that all of the chains in the surface are H chains with a 2× fluctuating brightness.

In order to see the detailed transformations near the step edge, empty-state STM images, obtained from small areas of 0.1 ML of Sb-deposited Si(5 5 12)-2×1 surface held at 600 °C, are presented in Figs. 3(c) and 3(d). In Fig. 3(c), the step edge is either a double-period (225) facet as shown inside segment "3" or a double-period (113) facet with a new chain as shown inside segment "4." This double-period (225) subunit is a resulting structure of consecutive switching between (225) and (337) subunits at the upper terrace, while the lower (337) terrace is not expanding. In segment 4, as

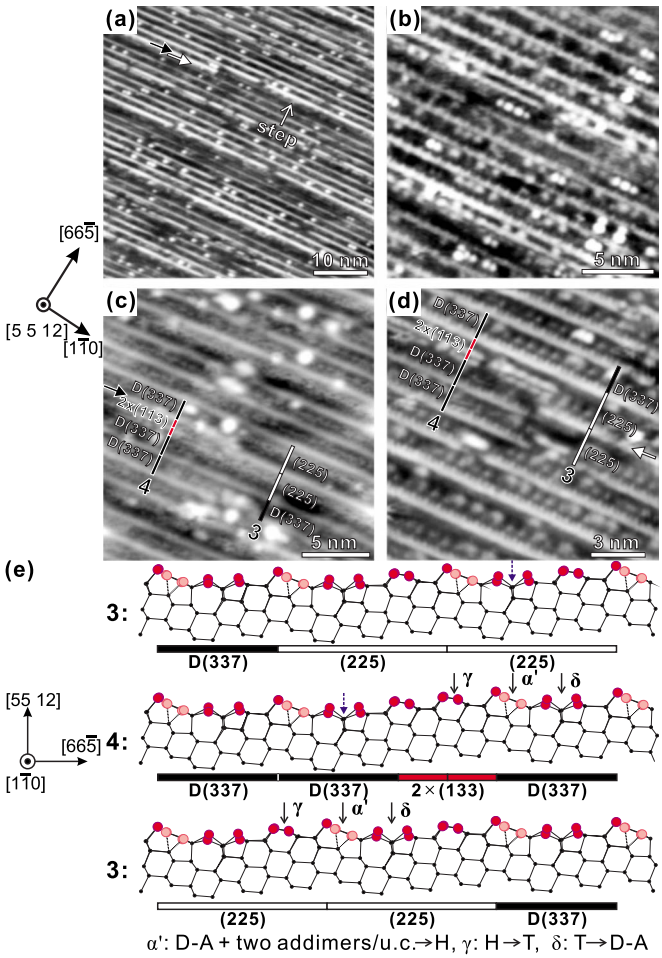

FIG. 3. (Color online) STM images obtained from the Si(5 5 12)-2×1 surface deposited with Sb at substrate temperature of 600 °C and corresponding structural models. (a) 0.05 ML Sb/Si(5 5 12)-2×1. Filled-state topographic image. Size: 50×50 nm^2, I_t=0.5 nA, and V_{sample}=−2.6 V. (b) 0.05 ML Sb/Si(5 5 12)-2×1. Empty-state topographic image. Size: 20×20 nm^2, I_t=0.5 nA, and V_{sample}=+1.3 V. (c) 0.1 ML Sb/Si(5 5 12)-2×1. Empty-state topographic image. Size: 20×20 nm^2, I_t=0.5 nA, and V_{sample}=+2 V. (d) 0.1 ML Sb/Si(5 5 12)-2×1. Empty-state topographic image. Size: 20×20 nm,[2] I_t=0.5 nA, and V_{sample}=+1.4 V. Arrows in (c) and (d) point the growth direction of new H chains. (e) Side-view models showing mutual transformation between 3 and 4 while the upper terrace is expanding.

designated by a black arrow inside the image, the additional chain has been formed on one of the (225) subunits which is adjacent to the upper (337) terrace. Utilizing the atomic structures of (225) and D(337) subunits shown in Fig. 1(e), the atomic structure corresponding to segment 3 is shown in the first row of Fig. 3(e). In segment 3, two dimers per unit cell are added to the (225) subunit adjacent to the upper (337) terrace [indicated by a dotted arrow in the first model of Fig. 3(e)] to form a new H chain and expand the upper (337) terrace by one unit, which corresponds to segment 4 in Fig. 3(c). The corresponding structural model is shown in the second row of Fig. 3(e). Different from the model, 2, shown in Fig. 2, the new chain is not a π chain but an H chain, since

a D(337) is newly formed instead of a T(337). Hence, formation of this new H chain is designated by α' in order to differentiate it from α shown in Fig. 2(b). On the other hand, the other accompanying transformations, γ and δ, are identical to those shown in Fig. 2(b). It can be clearly identified that the step between (337) terraces shown in Fig. 3 is a double-period (113) step composed of consecutive T rows. A similar (113) step composed of T row structures was also observed at the beginning of the (113) faceting during the homoepitaxy of Si(5 5 12)-2×1 held at 500 °C.[10] Therefore, these results confirm the deduction that the resultant surface faceting to the D(337) terraces with double-period (113) steps shown in Figs. 3(a) and 3(b) is due to indirect Si deposition.

For different Sb coverages (i.e., 0.05 and 0.1 ML), four surfaces shown in Figs. 3(a)–3(d) keep the similar terrace width and double-period (113) steps, which implies that two kinds of structures shown in 3 and 4 are reversible with an additional chain structure as shown in Fig. 3(d). As indicated by a white arrow in Fig. 3(d), through forming a new chain on the D-A site in the D(337) unit of the lower terrace adjacent to the (113) step indicated by a dotted arrow in the second model of Fig. 3(e), two consecutive (225) subunits corresponding to the third model in Fig. 3(e) are recovered. As a result, the double-period (225) step moves to the $[\bar{6}\bar{6}5]$ direction, as can be seen in the comparison of the first and third models of Fig. 3(e). In this reverse process, the identical transformations α', β, and γ are also employed. Such consecutive mutual transformations between 3 and 4 result in the expansion of the upper terrace and contraction of the lower terrace. Even though the expansion of the upper terrace has been divided into two processes, as indicated by two parallel arrows in Fig. 3(a), transformations 4→3 (white arrow) and 3→4 (black arrow) happen simultaneously in general. Due to a similar expansion occurring at the other end of the lower terrace at the same time, the terrace will keep a similar width for different Sb coverages as shown in Figs. 3(a)–3(d).

Even though the same Si atoms are deposited by either outer Si source in Si homoepitaxy[10] or by indiffused Sb replacing Si atoms in the present study, the resulting surfaces turn out to be quite different. The surface free energy near the direction of (5 5 12) is originally isotropic, but indiffused Sb atoms bonding with subsurface Si generate tensile stress to break the delicate stress balance of the high-index Si surface. This causes the surface free energy to be anisotropic, which results in faceting. Hence, the original Si(5 5 12)-2×1 surface, corresponding to the mixture of three (337) subunits and one (113) subunit, becomes faceted to (337) terraces with an about six-period width and double-period (113) steps. Similar faceting induced by metal adsorbates was also reported previously.[6,7]

C. Growth and saturation of Sb nanowires on the Si(337) terrace

In Fig. 4(a), a filled-state STM image obtained from 0.15 ML of Sb-deposited Si(5 5 12)-2×1 held at 560 °C is shown. In Fig. 4(a), a feature designated by arrow "S" is

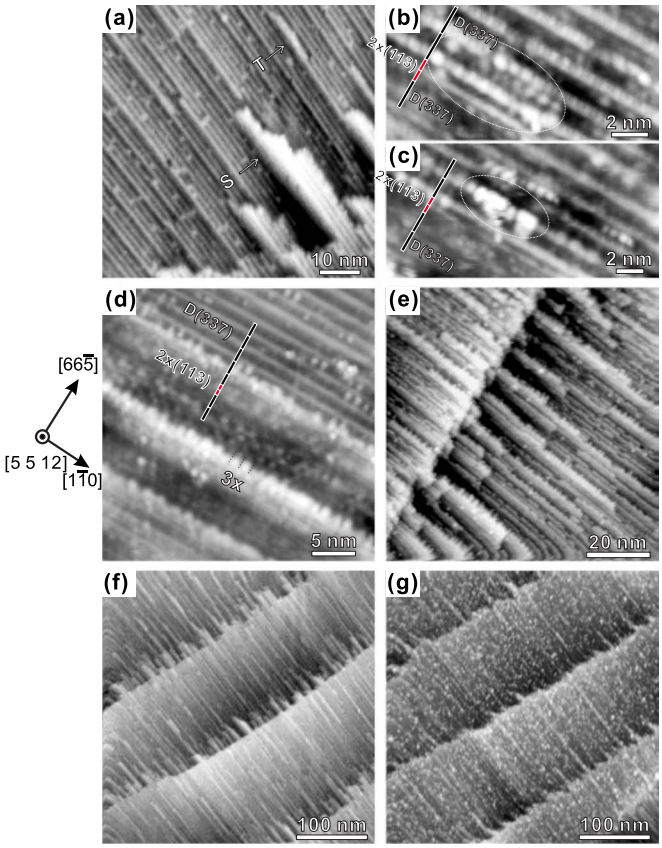

FIG. 4. (Color online) Topographic STM images of Sb-deposited Si(5 5 12)-2×1 at elevated temperatures. (a) 0.15 ML, T_{sub}: 560 °C, size: 80×80 nm^2, I_t=0.5 nA, and V_{sample}=−2.4 V. (b) 0.18 ML, T_{sub}: 600 °C, size: 15×7.5 nm^2, I_t=0.5 nA, and V_{sample}=+1.3 V. (c) 0.18 ML, T_{sub}: 600 °C, size: 20×10 nm^2, I_t=0.5 nA, and V_{sample}=+1.4 V. (d) 0.18 ML, T_{sub}: 600 °C, size: 30×30 nm^2, I_t=0.5 nA, and V_{sample}=+1.7 V. (e) 0.2 ML, T_{sub}: 600 °C, size: 80×80 nm^2, I_t=0.5 nA, and V_{sample}=+1.7 V. (f) 0.45 ML, T_{sub}: 600 °C, size: 400×400 nm^2, I_t=0.5 nA, and V_{sample}=+1.7 V. (g) 1 ML, T_{sub}: 600 °C, size: 400×400 nm^2, I_t=0.5 nA, and V_{sample}=+1.7 V.

grown from a facet which is not parallel to the $[1\bar{1}0]$ direction. It consists of (337) and (113) facets with the same structures as Si ones, so it can be deduced that the element of these elongated features grown from the vertical steps is not Sb but Si. On the other hand, another new feature designated by arrow "T" starts to grow along the double-period (113) step in the terrace.

In Figs. 4(b)–4(d), empty-state STM images, obtained from 0.18 ML of Sb-deposited Si(5 5 12)-2×1 held at 600 °C, are shown. Figures 4(b) and 4(c) show the initial stage of a new structure induced by Sb deposition of more than 0.15 ML. Inside the oval of Fig. 4(b), new features brighter than surrounding H chains having fluctuating brightness are shown in the H chains of the upper (337) terrace neighboring a 2×(113) facet. These features are thought to be Sb atoms which substituted Si atoms in the H chains. Inside the oval of Fig. 4(c), bright protrusions are shown, which are thought to be the second layer of Sb atoms on the Sb atoms which substituted Si atoms. As can be seen in Fig.

4(d), a nanowire has been formed along the upper step edge, where Sb substitution for Si occurs and the second Sb layer is formed. As shown in Fig. 4(e), when the depositing amount increases to 0.2 ML, these 1D nanowires grow along either $[1\bar{1}0]$ or $[\bar{1}10]$ direction. The spacing between adjacent Sb wires tends to keep the same width, about 10 nm, as that of the (337) terraces. The atomic structure of growing nanowires is ordered and different from that of the Si facet formed during homoepitaxy on Si(5 5 12)-2×1.[10] The highest part of 1D nanowires has a 3× periodicity along the $[1\bar{1}0]$ direction, as marked with dotted lines in Fig. 4(d). Therefore, this newly formed 1D feature is a facet composed of Sb atoms. As soon as Sb indiffusion saturates, the Sb starts to form the 1D feature along the upper step edge, which has an adsorption site for Sb dimers such as the D-A row in a D(337) subunit as well as a diffusion barrier across the step, that is, the Ehrlich-Schwoebel (ES) barrier.[22,23] It is well known that this ES barrier affects the growth mode during deposition of external atoms on the substrate with a step or a facet like that of the present case.[24,25]

In Figs. 4(f) and 4(g), STM images, obtained after 0.45 and 1 ML of Sb deposition on Si(5 5 12)-2×1 held at 600 °C, are shown. The isolated 1D Sb nanowires are formed up to 0.45 ML of Sb coverage, and then the deposited Sb atoms are clustered at 1 ML of Sb coverage. Once Sb clustering initiates, no specific structural change is detected with additional Sb atoms. In Fig. 4(f), most of the (113) steps have been saturated by Sb wires and few preferential adsorption sites are left for additional growth of 1D Sb wires. In other words, the strain laid on the (113) steps has been released by adsorbed Sb atoms, so that additionally deposited Sb atoms cannot find any preferential adsorption sites but cluster for themselves, which results in random distribution on the surface. Then, the surface reaches at the equilibrium state between deposition and re-evaporation. In the present experiment, Sb was evaporated from the source held at 330 °C. Considering the substrate temperature, 600 °C, and the evaporation source temperature, 330 °C, re-evaporation from Sb clusters on the substrate is not surprising. This is the reason why the density of Sb cluster does not increase with extended Sb deposition in the present experiment. According to Kumar *et al.*, the saturation of Auger peak intensity ratio of Sb relative to Si on Sb/Si(5 5 12) deposited at 680 °C is also attributed to the fact that the Sb sticking coefficient on the first Sb ML reduces to zero around this temperature.[8] The similar saturation or re-evaporation of adsorbed Sb on Si(111) (Ref. 26) or Si(001) (Refs. 20 and 27) had also been reported.

IV. CONCLUSION

In the present study, the utility of the Si(5 5 12)-2×1 surface as a template has been tested. At the initial stage of Sb adsorption on the Si(5 5 12)-2×1 substrate held at 600 °C, deposited Sb atoms diffuse into the subsurface. Such Sb indiffusion causes the substituted Si atoms to be outdiffused and adsorbed on the preferential adsorption sites of the surface. Such indirect Si homoepitaxy results in faceting to the (337) terraces and (113) facets, being different from the result of direct Si homoepitaxy, where the original Si(5 5 12)-2×1 surface is recovered after a cycle of homoepitaxy.[10] This contrasting result is due to the surface tensile stress caused by indiffused Sb atoms. In the present indirect Si homoepitaxy, only one set of structural transformations takes place simultaneously as follows: Two Si dimers per unit cell, outdiffused from the subsurface, are adsorbed on the D-A row in the (225) subunit and form a new π chain. This newly formed chain generates the surface stress along the $[\bar{6}\bar{6}5]$ direction acting as a compressive stress to the neighboring H chain to be converted to a T row and also acting as a tensile stress to the π chain and the T row in the neighboring T(337) to be converted to an H chain and a D-A row in a D(337). Such a set of transformations results in the mutual exchange between a (337) subunit and a (225) subunit, which corresponds to the movement of the (225) subunit along the $[\bar{6}\bar{6}5]$ direction. In the present experiment, it has been observed that bunching of two sequential (225) subunits advances the most stable configuration, combination of a (337) terrace with an about six-period width and a (113) step with a two-period width. However, when Sb indiffusion terminates due to depletion of subsurface Sb sites, such indirect Si deposition also terminates and the arriving Sb atoms are continuously adsorbed along the upper (113)-step edge on the surface until the available (113) steps are also depleted. Finally, the additional Sb atoms cluster for themselves until the surface reaches at an equilibrium state between Sb atoms arriving at the surface and Sb atoms desorbing from the surface.

For ideal nanowire fabrication on the Si(5 5 12)-2×1 template, the present experimental result suggests that it is the most critical to find proper metals and temperature window which will not cause interdiffusion, since intermixing between adsorbed species and the substrate, even though its amount is much less than 1 ML, can result in faceting of the substrate to a nonideal template.

ACKNOWLEDGMENT

This work was supported by Korea Research Foundation Grant (KRF-2006-005-J00301).

*seojm@chonbuk.ac.kr; http://nano.chonbuk.ac.kr

[1] A. A. Baski, S. C. Erwin, and L. J. Whitman, Science **269**, 1556 (1995).

[2] J. Liu, M. Takeguchi, H. Yasuda, and K. Furuya, J. Cryst. Growth **237-239**, 188 (2002).

[3] S. Jeong, H. Jeong, S. Cho, and J. M. Seo, Surf. Sci. **557**, 183 (2004).

[4] H. Kim, H. Li, Y.-Z. Zhu, J. R. Hahn, and J. M. Seo, Surf. Sci.

601, 1831 (2007).
[5] Q. Chen and N. V. Richardson, Prog. Surf. Sci. **73**, 59 (2003).
[6] A. A. Baski, K. M. Saoud, and K. M. Jones, Appl. Surf. Sci. **182**, 216 (2001).
[7] S. Cho and J. M. Seo, Surf. Sci. **565**, 14 (2004).
[8] M. Kumar, V. K. Paliwal, A. G. Joshi, Govind, and S. M. Shivaprasad, Surf. Sci. **596**, 206 (2005).
[9] M. Kumar, Govind, V. K. Paliwal, A. G. Vedeshwar, and S. M. Shivaprasad, Surf. Sci. **600**, 2745 (2006).
[10] H. Kim, Y. Cho, and J. M. Seo, Surf. Sci. **583**, 265 (2005).
[11] *User's Guide To Autoprobe VP* (Park Scientific Instruments, Sunnyvale, CA, 1996), Chap. 4.
[12] J. R. Power, O. Pulci, A. I. Shkrebtii, S. Galata, A. Astropekakis, K. Hinrichs, N. Esser, R. Del Sole, and W. Richter, Phys. Rev. B **67**, 115315 (2003).
[13] E. Martínez-Guerra, G. Falkenberg, R. L. Johnson, and N. Takeuchi, Phys. Rev. B **73**, 075302 (2006).
[14] A. A. Saranin, A. V. Zotov, V. G. Kotlyar, V. G. Lifshits, O. Kubo, T. Harada, T. Kobayashi, N. Yamaoka, M. Katayama, and K. Oura, Jpn. J. Appl. Phys., Part 1 **40**, 6069 (2001).
[15] M. Jiang, X.-Y. Zhou, B.-X. Li, and P.-L. Cao, Phys. Rev. B **60**, 8171 (1991).
[16] Y.-J. Ko, K.-H. Park, J. S. Ha, and W. S. Yun, Phys. Rev. B **59**, 4588 (1999).
[17] M. A. Boshart, A. A. Bailes III, and L. E. Seiberling, Phys. Rev. Lett. **77**, 1087 (1996).
[18] L. H. Chan and E. I. Altman, Phys. Rev. B **63**, 195309 (2001).
[19] S. Hasegawa, R. G. Ryland, and E. D. Williams, Appl. Phys. Lett. **65**, 2609 (1994).
[20] B. Garni, I. I. Kravchenko, and C. T. Salling, Surf. Sci. **423**, 43 (1999).
[21] A. A. Saranin, A. V. Zotov, V. G. Kotlyar, V. G. Lifshits, O. Kubo, T. Harada, T. Kobayashi, N. Yamaoka, M. Katayama, and K. Oura, Phys. Rev. B **65**, 033312 (2001).
[22] C. Roland and G. H. Gilmer, Phys. Rev. Lett. **67**, 3188 (1991).
[23] S. Kodiyalam, K. E. Khor, and S. Das Sarma, Phys. Rev. B **53**, 9913 (1996).
[24] I. Markov, Phys. Rev. B **54**, 17930 (1996).
[25] T. Sekiguchi, S. Yoshida, and K. M. Itoh, Phys. Rev. Lett. **95**, 106101 (2005).
[26] V. K. Paliwal, A. G. Vedeshwar, and S. M. Shivaprasad, Phys. Rev. B **66**, 245404 (2002).
[27] V. K. Paliwal, A. G. Vedeshwar, and S. M. Shivaprasad, Surf. Sci. **540**, L617 (2003); V. K. Paliwal and S. M. Shivaprasad, *ibid.* **561**, L207 (2004).